

The effect of service-temperature exposure on the tensile properties of Ti-1421/SiC metal matrix composites

A. M. RITTER, P. DUPREE

GE Corporate Research Development, Po Box 8, K-1, MB241, Schenectady, New York, NY 12301, USA

Composites consisting of a Ti–14Al–21Nb (wt %) aluminide matrix and SCS-6 SiC fibres were fabricated by plasma-spraying and hot-isostatic-pressing. The room temperature longitudinal tensile properties were evaluated after processing and after isothermal and cyclic exposure in air and in argon. The isothermal ages were performed at 760 °C, and the thermal cycle was from room temperature to 760 °C, which is the projected service temperature for Ti-aluminide-based composites. Some loss of tensile strength occurred after isothermal and cyclic exposure for long times (8 to 12 weeks) in argon, with no apparent difference in behaviour between the isothermal and cyclic samples. Substantial degradation in tensile properties was seen after isothermal exposure in air, while a much more severe loss in properties occurred after cycling in air. In the isothermal samples exposed in air, degradation in properties was associated with surface embrittlement of the matrix, with the longitudinal room temperature tensile strength decreasing linearly with increasing thickness of the embrittled zone. During air-cycling, this effect was enhanced by a rapid decrease in the strength of the SCS-6 fibre, and an increase in the amount of fibre breakage. Isolating the fibres from direct contact with the environment resulted in a decrease in the amount of composite strength degradation after air-cycling.

1. Introduction

Titanium and titanium aluminide/SiC fibrous composites are currently under consideration for use in aircraft engines as a means to increase the thrust-to-weight ratio, and their fabrication and microstructure are under study by several groups [1–8]. One class of matrix alloys which has been of interest is based on Ti₃Al (alpha-2), and of this alloy type, Ti–14Al–21Nb (wt %), or Ti-1421, has been extensively studied. The SiC fibre that has been most frequently used in this matrix in work presented to date is the SCS-6 SiC fibre manufactured by Textron Specialty Materials. This fibre, which has a carbon core on which beta-SiC has been deposited by chemical vapour deposition (CVD), has layers of Si-rich graphite as a protective coating [9]. Chemical interaction of this coating with Ti-base matrices [10, 11] and the strength and effect of the fibre/coating/matrix interface on mechanical properties [12] have been well characterized.

Ti-1421/SCS-6 composites can exhibit high stiffness and strength relative to the unreinforced matrix material, both at room temperature and elevated temperature, and extensive characterization of the tensile properties has been performed to assess property development and variability [5, 13, 14], as well as the effects of processing methods on properties [15]. Some consideration has also been given to the microstructural stability and mechanical behaviour of these

materials after thermal exposure at the proposed operating temperature [10, 13, 16–18], and property degradation has been reported [13, 16, 17] when thermal exposure was done in air.

This study presents data from Ti-1421/SiC composites which were isothermally and cyclically exposed in argon and air at service temperatures, and considers mechanisms for the observed behaviour.

2. Experimental procedure

The composites were fabricated by RF plasma-spraying Ti alloy powder onto drums wound with SiC fibres [1]. The powders were fabricated by the plasma-rotating-electrode process (PREP) at Nuclear Metals. The alloy used was Ti-1421, and the powder size fraction was (–80 +140). The SCS-6 SiC fibre was manufactured by Textron Specialty Materials, and was wound on the drums at an average fibre spacing of 128 per inch. Interstitial analysis was done on the plasma-sprayed tapes. Consolidation of 4-ply composites for testing was by hot-isostatic-pressing, and panels were fully consolidated, with no porosity. Panels with a range of fibre volume fractions (16–33%) were fabricated in order to study the effect of fibre content. Panels of fibreless material were made by plasma-spraying the Ti-1421 powder onto drums, and HIPing the fibreless foils using the same conditions as for the composites.

Room temperature longitudinal (0°) tensile properties were measured for each of the composite panels. Room temperature tensile properties were also obtained on the fibreless panels. The tensile samples were 10.16 cm long by 1.016 cm wide, and were straight-sided. Tensile testing was done on samples with as-fabricated surfaces, i.e. no grinding was done to remove a Mo-enriched layer present due to interaction of the Ti-1421 matrix with the Mo foil in the HIP can. Longitudinal composite samples were aged isothermally in argon and in air for times up to 2016 h at 760 °C. Thermal cycling in argon and in air was done from room temperature to 760 °C. The cycle was 20 min to heat the samples, 30 min at temperature, and 30 min to cool the samples to room temperature. Samples from fibreless panels were isothermally exposed at 760 °C. All samples were tensile tested without any surface preparation to remove oxide. Tensile testing was done at room temperature. All argon exposures were done with the samples encapsulated in quartz tubes which were back-filled with argon. The samples were wrapped with Ta foil, and a small piece of yttrium was placed in the tube to get any residual oxygen.

Samples were also made in which the fibres were completely isolated from direct contact with the environment, by HIPing a layer of matrix around the sides and ends of a straight-sided sample. These buried-fibre samples were cycled in air to 760 °C, and then tensile-tested at room temperature.

The as-HIP and exposed specimens were examined using optical microscopy on metallographic samples etched with Kroll's solution (100 ml water, 5 ml nitric acid, and 2 ml hydrofluoric acid). Scanning electron microscopy (SEM) was performed on the fracture surfaces of the tensile samples. Samples were also examined in the analytical electron microscope (AEM), and were prepared by ion-milling.

Fibres were tensile tested in the as-received, as-plasma-sprayed and as-HIP condition. The fibres were removed from the plasma-sprayed tapes and HIPed panels by dissolving the matrix in a solution of 400 ml nitric acid/400 ml water/40 ml hydrofluoric acid at a temperature of 50 °C. Fibres were also etched

from Ar-exposed and air-exposed composites, and were then tensile tested. The amount of fibre breakage after HIP and after exposure was evaluated semi-quantitatively by measuring the weight of extracted fibres which were 7.62–10.16 cm long (assumed to be unbroken), and those that were less than 7.62 cm long.

3. Results and discussion

3.1. Fibreless Ti-1421 panels

Four Ti-1421 panels were evaluated in this study, and the room temperature tensile properties for these panels are shown in Table I. Since there was some variability in the tensile elongation from panel to panel, presumably because of variation in interstitial content, data from all the panels are presented instead of average properties. The microstructure consisted of an alpha-2 (Ti₃Al) matrix with varying amounts of beta-phase or transformed beta-phase. The transformed beta-phase in the as-HIP samples consisted of laths of beta plus orthorhombic Ti₂AlNb, and occasionally of alternating alpha-2/beta laths. Isothermal ageing in argon at 760 °C resulted in destabilization of the orthorhombic phase in these regions, resulting in a mixture of beta and alpha-2. This had no apparent effect on the room temperature tensile properties. However, exposure in air at this temperature resulted in considerable degradation in strength and ductility. The ductility was affected after shorter exposure times, with as little as 4 h in air showing a significant decrease in ductility.

3.2. Ti-1421/SiC panels

The microstructure of a typical as-HIP composite panel is shown in Fig. 1. As in the case of the fibreless panels, the matrix was alpha-2, with dark-etching regions of beta-phase and transformed beta-phase. There was a beta-depleted region near the SCS-6 fibres (Fig. 1b), as has been reported by several researchers [3,4,7], and this region tended to crack during consolidation, presumably during cool-down from the HIP temperature. A reaction zone between the SCS-6 carbon coatings and the matrix formed

TABLE I Room temperature tensile properties of TI-1421

Panel	Condition	0.02% YS	UTS	Total strain	Plastic strain
RF1090	as-HIP	540 MPa	650 MPa	1.05%	0.37%
	672 h/Ar	590	600	1.04	0.44
	1344 h/Ar	580	600	1.53	0.94
	672 h/air	–	440	0.44	0.01
	1344 h/air	410	430	0.44	0.02
RF1589	as-HIP	470	670	0.97	0.27
	672 h/air	430	510	0.51	0.04
RF1213	as-HIP	540	670	1.53	0.89
	0.5 h/air	590	650	1.69	1.01
	1 h/air	520	640	0.97	0.37
	4 h/air	440	620	0.67	0.11
RF1622	as-HIP	700	740	1.29	0.61
	4 h/air	680	730	1.07	0.31
	25 h/air	680	730	1.02	0.28

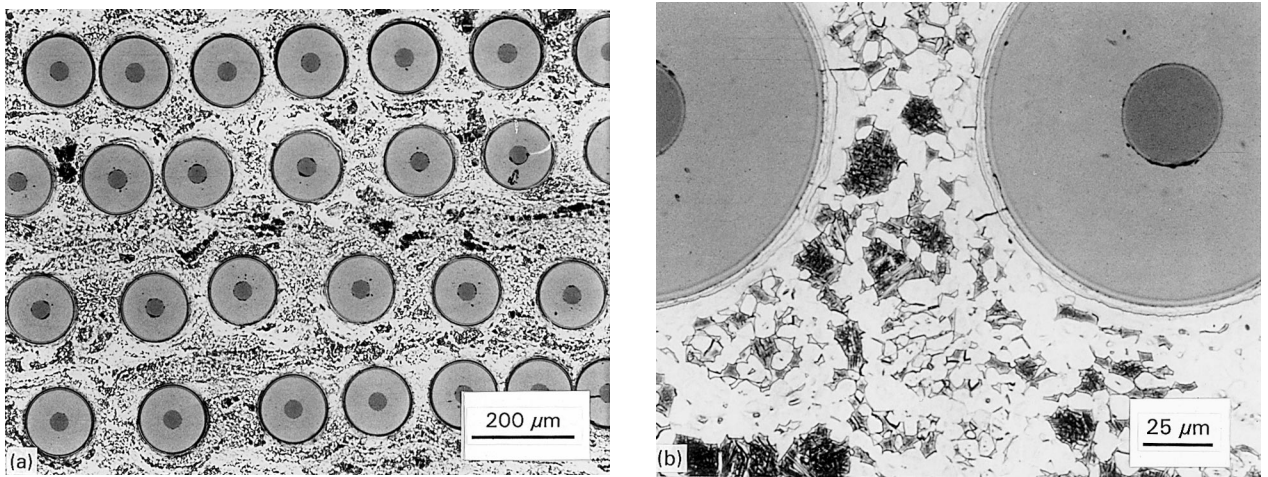


Figure 1 Optical micrograph showing (a) typical microstructure of as-HIP Ti-1421/SiC, and (b) beta-depleted region near fibre, with microcracks radiating from reaction zone.

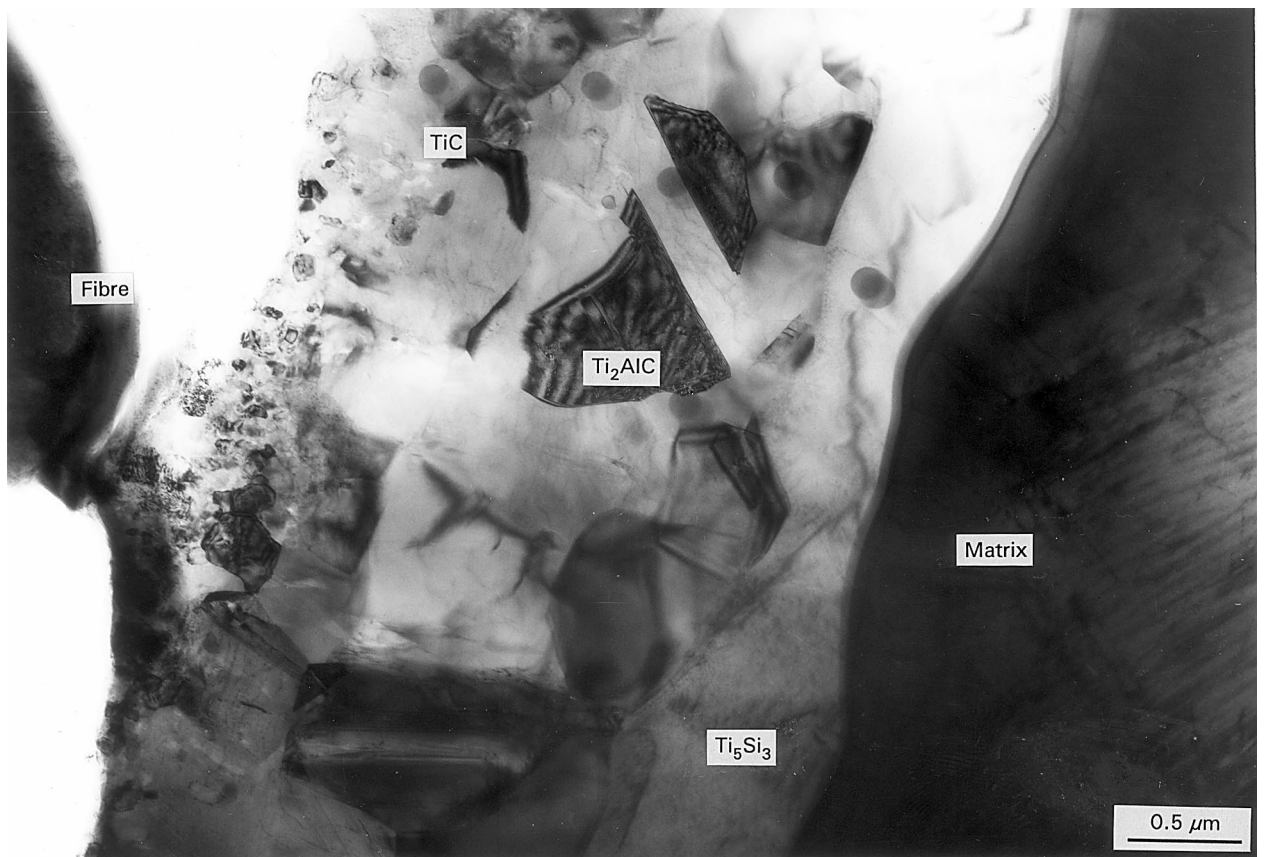


Figure 2 Transmission electron micrograph of reaction zone between fibre coating and matrix in as-HIP Ti-1421/SCS-6 composite.

during HIP, and consisted of three regions [5], as shown in Fig. 2. There was a band of Ti-rich MC carbides next to the fibre coatings, and the grain size in this region increases with distance from the fibre. Next to the MC band was a region of Ti_2AlC , and the region adjacent to the metal matrix consisted of $(Ti, Nb)_5Si_3$ precipitates.

There was considerable panel-to-panel variability in as-HIP composite tensile properties in all of the Ti-1421/SiC material. Much of this variability can be attributed to differences in fibre strength after processing. This is illustrated in Fig. 3. In this, the compo-

site tensile strength is plotted against volume fraction SiC \times HIP fibre strength, a factor which is equivalent to the rule-of-mixtures contribution of the fibre, in the absence of residual stresses. Comparison of mean fibre strengths from HIPed panels with as-received fibre data showed that some strength degradation had occurred during HIP. Measurement of the tensile strengths of as-received fibres on a number of spools showed a range in strength of 3100–5200 MPa, with a mean strength for all spools of \sim 4100 MPa. Fibres extracted from plasma-sprayed tapes showed no degradation in strength. After HIP consolidation,

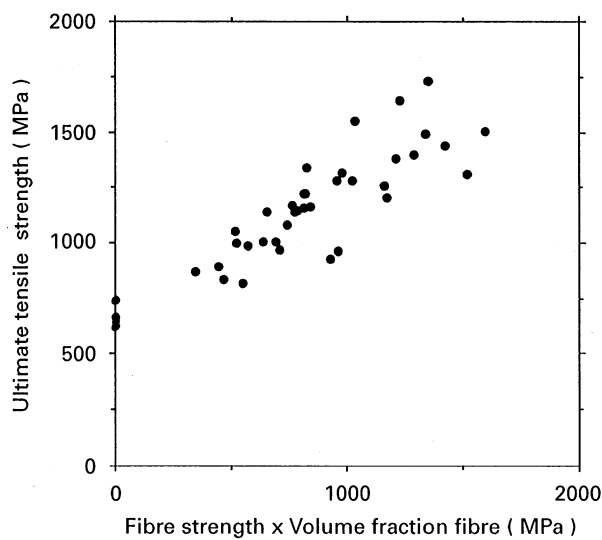


Figure 3 Room temperature ultimate tensile strength as a function of HIP fibre strength \times volume fraction SiC for Ti-1421/SiC longitudinal composites with 13 to 39 vol% SiC.

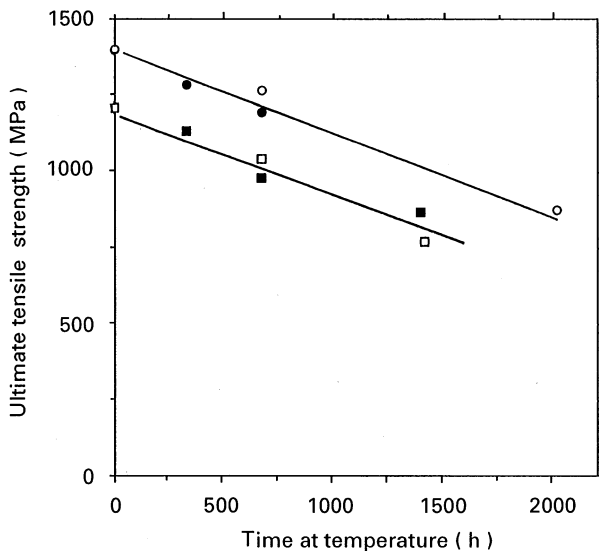


Figure 4 Room temperature ultimate tensile strength of Ti-1421/32-22SiC longitudinal composites measured after isothermal and cyclic exposure in argon at 760 °C. Data are from two different panels shown in legend. Cycle is 20 min heating, 30 min at 760 °C, and 20 min cooling. Key: \circ RF971, isothermal; \bullet RF971, cyclic; \square RF1256, isothermal; \blacksquare RF1256, cyclic.

however, there was a larger range of average fibre strengths from different panels (2100–5200 MPa), and the mean fibre strength for all samples had decreased to \sim 3400 MPa. This decrease in strength is associated with the decrease in the SCS-6 fibre coating thickness, due to reaction with the matrix during HIP [19].

There was some decrease in composite strength after both isothermal ageing and cycling in argon (Fig. 4). Isothermal and cyclic ageing in argon had equivalent effects on properties. Work by other researchers [17,18] did not show significant strength loss when cycling Ti-1421/SCS-6 in an inert environment. The total time at elevated temperature was considerably longer for the thermal cycle used in the current study, and this may account for the difference between other results and the data presented here.

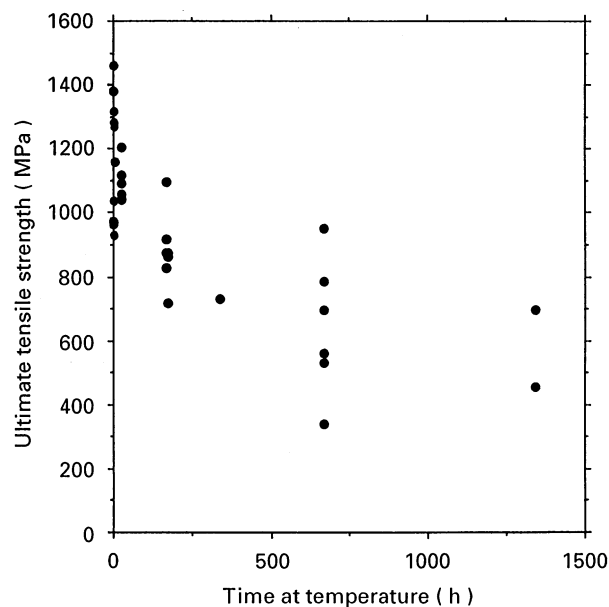


Figure 5 Room temperature ultimate tensile strength of Ti-1421/24-26SiC longitudinal composites measured after isothermal exposure in air at 760 °C. Data are from seven different panels.

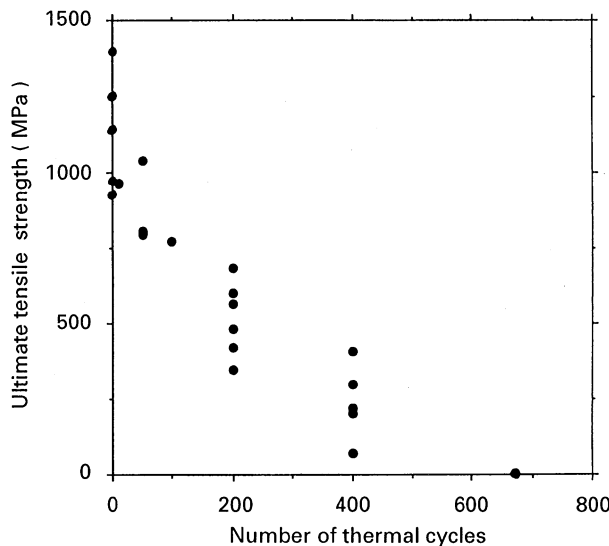


Figure 6 Room temperature ultimate tensile strength of Ti-1421/21-33SiC longitudinal composites measured after cyclic exposure in air to 760 °C. Data are from five different panels. Cycle is 20 min heating, 30 min at 760 °C, and 20 min cooling.

Isothermal exposure in air at 760 °C caused rapid strength degradation in samples from some panels, but much less property loss in others, as seen in Fig. 5. The source of this variability will be discussed later. Thermal cycling in air at 760 °C affected all of the panels in an approximately similar fashion (Fig. 6). Thermal cycling in air at 760 °C resulted in much more rapid degradation than isothermal ageing. This rapid drop in composite strength is similar to data [16,17] from Ti-1421/SiC panels cycled in air at 815 °C. Isothermal and cyclic exposure in air at 760 °C also resulted in large decreases in tensile elongation.

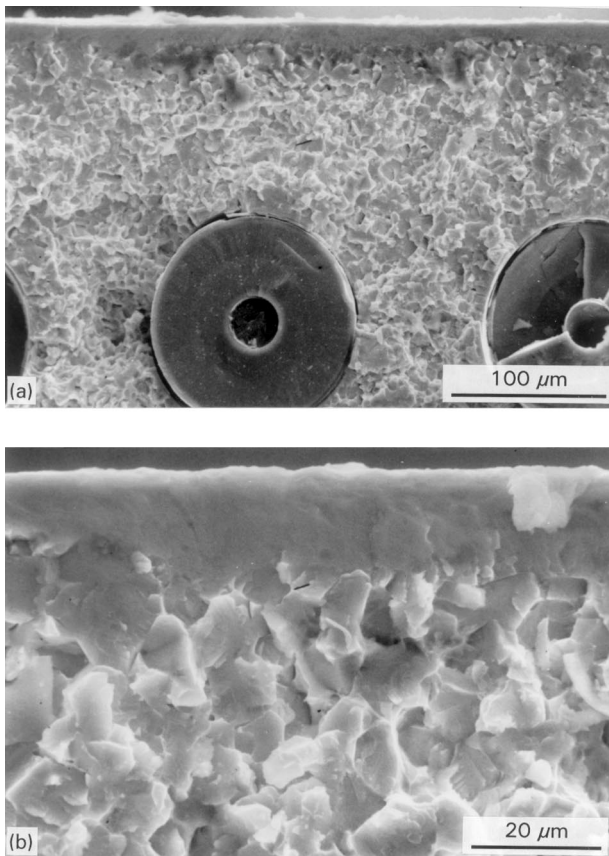


Figure 7 Scanning electron micrographs of fracture surface of Ti-1421/SCS-6 room temperature tensile samples tested after exposure in air at 760 °C, showing flat cleaved zone corresponding to embrittled region of matrix surface.

3.3. Mechanisms for property degradation

3.3.1. Matrix surface embrittlement

The presence of an embrittled surface layer is expected to be deleterious, since work on unreinforced Ti-6242 [20] and in Ti-1421 [21] has shown that the presence of an alpha phase is damaging to the overall ductility of the alloy. It has also been shown [7], that a critical level of matrix ductility ($\sim 2\text{--}3\%$) is required to attain rule-of-mixtures properties in Ti-base composites. The effect of surface embrittlement on matrix and composite properties has been evaluated quantitatively by measuring the extent of the embrittled region from fracture surfaces of tensile specimens. The embrittled region tends to be a flat cleaved zone, clearly distinguishable from the mixed mode (cleavage + microvoid coalescence) fracture of the unaffected matrix (Fig. 7). The depth of this cleaved zone was measured for all of the air-exposed samples, and varied in an approximately linear fashion with the square root of time at temperature (Fig. 8). There was a large amount of sample-to-sample variability in these measurements. As seen in Fig. 9, the composite strength decreased linearly with increasing depth of this embrittled region. The average strength of a composite with a specific cleaved zone thickness was generally higher for the isothermal samples than for the air-cycled samples. This indicated that some damage other than surface embrittlement had occurred in the air-cycled samples.

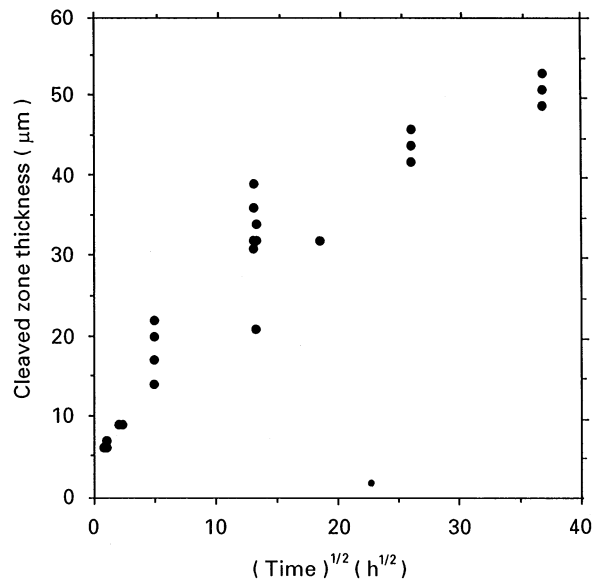


Figure 8 Cleaved zone thickness as a function of the square root of time at temperature for Ti-1421/SCS-6 exposed isothermally at 760 °C, as measured from the fracture surface of room temperature tensile samples.

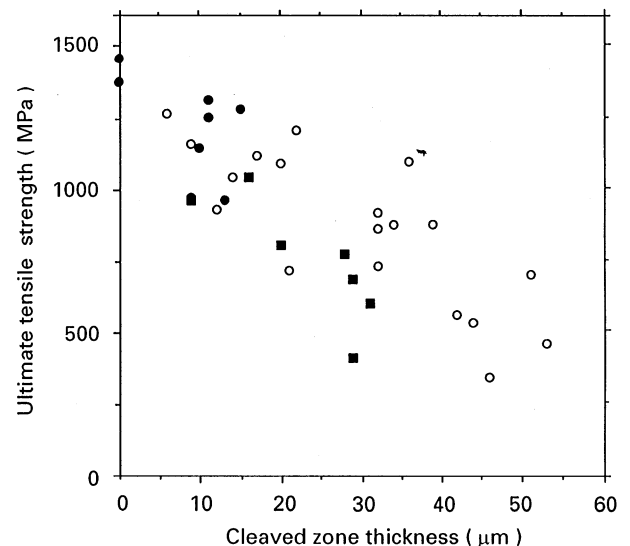


Figure 9 Room temperature ultimate tensile strength of as-HIP and air-exposed Ti-1421/SCS-6 composites as a function of cleaved zone thickness. Key: ● as-HIP; ○ isothermal; ■ cycled.

In isothermally-exposed samples, the strength degradation observed was probably due to surface cracking during tensile testing. For example, in Ti-1421/SiC tensiles there were no extended matrix cracks in as-HIP material after testing (Fig. 10a), while in a tested tensile sample exposed in air for 672 h at 760 °C, there were numerous matrix cracks perpendicular to the applied stress (Fig. 10b), as has also been observed [21] in thermally-exposed Ti-1421 panels. These cracks originate in the embrittled surface layer. In the air-cycled samples, the embrittled surface regions cracked during cycling and during tensile testing, as has been reported [16,17] for Ti-1421/SiC panels cycled in air to 815 °C. Surface cracks which initiated during cycling then propagated into the matrix during further cycling, embrittling the

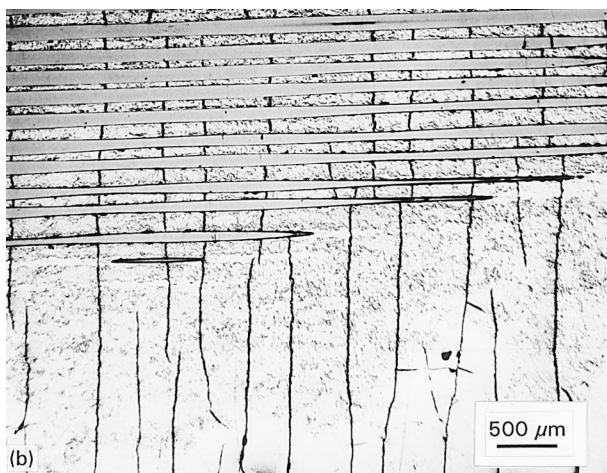
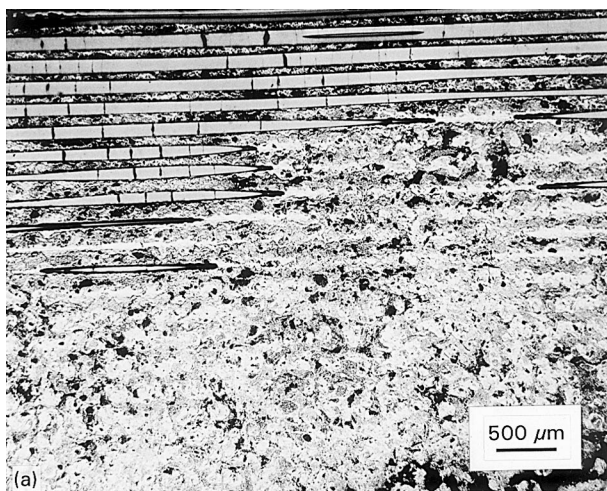


Figure 10 Longitudinal sections of room temperature tensile sample. (a) As-HIP, and (b) tested after isothermal exposure in air at 760 °C. Cracks in matrix are perpendicular to applied stress, and initiated in embrittled surface during tensile test.

matrix regions adjacent to the cracks (Fig. 11). Since no stress was applied to the samples during cycling, crack propagation apparently occurred due to stresses arising from the thermal expansion mismatch between the SCS-6 fibres and the matrix, as has been reported by Revelos and Smith [17]. This cracking also contributed to the delamination of the fibre layers, as discussed below.

The cracking of an embrittled surface region, and the deleterious effects on composite strength detailed in this paper are similar to results for Ti-1421/SCS-6 which was coated with a brittle oxidation-resistant coating before thermal cycling [17]. In this case, the brittle coating cracked during air-cycling, and the cracks propagated into the composite, resulting in a more severe loss in strength than for air-cycled uncoated samples.

The large panel-to-panel variability in strength of the isothermal samples as a function of time at temperature (Fig. 5) was considerably reduced when the strength was plotted as a function of cleaved zone thickness. The range in the depth of embrittlement for any given time (Fig. 8) was of the order of 10 μm over the various samples examined. This variability in response of the different panels to formation of an

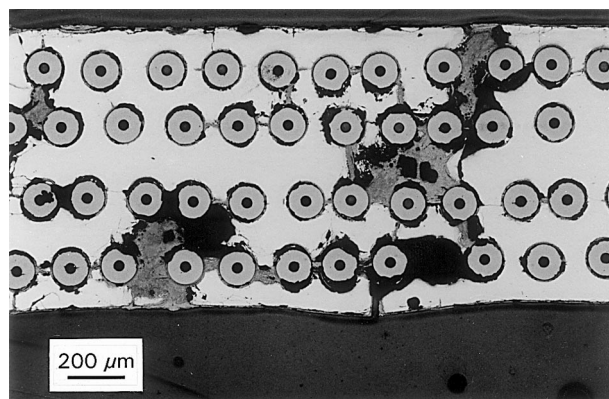


Figure 11 Cross-section of longitudinal Ti-1421/SCS-6 composite which was cycled in air to 760 °C for 672 cycles, showing matrix cracking which occurred during thermal cycling. Cycle is 20 min heating, 30 min at 760 °C, and 20 min cooling. Sample is as-cycled, without applied load.

embrittled region may account for the spread in the tensile data in Fig. 5. The reason for the panel-to-panel variation in cleavage zone thickness may be related to differences in Mo-enrichment on the panel surfaces. The Mo-rich regions are the result of diffusion of Mo into the matrix from the protective foil between the composite and the HIP can. Current practice in testing and thermally exposing these composites is to remove the Mo-rich region from the composite surface by grinding or by etching. However, this effect was not well-known at the time the samples in this study were fabricated and tested. The presence of the Mo-rich region can also affect the cracking mechanisms when composites are tested in creep [22].

3.3.2. Delamination of fibre layers

The samples cycled in air to 760 °C showed delamination of the fibre layers, as seen in Fig. 12. Delamination proceeded along the fibre/matrix interface, and was associated with regions of fibre coating oxidation. This oxidation started at the cut surface of the composite sample, where fibres and fibre coatings were exposed to the atmosphere. As the coating on a fibre near the surface was oxidized, delamination at the fibre/matrix interface occurred, and a crack was initiated in the matrix region within the fibre layer. As in the case of cracks originating in the embrittled surface of the matrix, the crack was presumably propagated by stresses arising from thermal expansion mismatch between the fibres and matrix. The presence of matrix cracks and fibre delamination resulted in a very low composite strength (~5–23 MPa).

In addition to oxidation of fibre coatings along delaminations, the coatings may be affected by oxygen transported down the fibre axis from the cut ends of the samples. Coating oxidation from sample ends has been seen in longitudinal sections of the isothermally exposed as well as cycled tensile samples. Fibre coating oxidation from cut ends and cut sides of samples could be limited by designing a part such that the fibres are completely buried in the matrix.

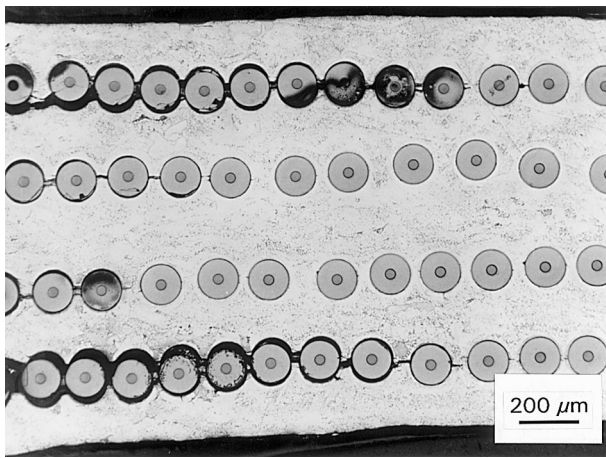


Figure 12 Cross-section of longitudinal Ti-1421/SCS-6 composite which was cycled in air to 760 °C, showing delamination of fibre layers proceeding from exposed and oxidized fibres at sample edge. Sample is as-cycled, without applied load.

TEM examination of SCS-6 coatings on fibres which had been exposed isothermally in air at 760 °C showed that they were no longer graphite with some SiC particles, as observed [12] for as-HIP fibres. Instead, the fibre coatings contained Si and O, and had presumably transformed to silica. The coatings were also very porous in appearance. These results are similar to observations [23] on fibres which had been aged in air in a Ti-base matrix for sufficient time to diffuse oxygen to the fibres.

To assess the overall effect on composite properties of isolating the fibres from the oxidizing environment, the buried-fibre samples were cycled in air to 760 °C and then tensile tested at room temperature. The results from these tests are shown in Fig. 13, which also shows the data from isothermally-exposed samples and from air-cycled samples. As can be seen, the air-cycled buried-fibre samples did not degrade as rapidly as the air-cycled samples which did not have the fibres shielded from direct contact with the environment. The air-cycled buried-fibre samples were at the lower end of the data band for the isothermally-exposed samples. This indicates that the buried-fibre samples may have experienced some damage during cycling, but that it was not as extensive as for the cycled samples with exposed fibres. The major effect on the fibres due to cycling with fibres exposed at sample ends and at sample edges appeared to be a decrease in strength and increase in fibre breakage, as discussed below.

3.3.3. Changes in fibre strength and fibre breakage

Composite strength degradation may be related to loss of fibre strength and fibre integrity. A major factor in the development of composite strength is the fibre strength after HIP, as was shown in Fig. 3. Loss of fibre strength due to fibre/matrix interaction or to oxidation of the fibre coatings would therefore result in decreased composite strength. In addition, the ultimate tensile strength of Ti-1421/SiC is sensitive to the

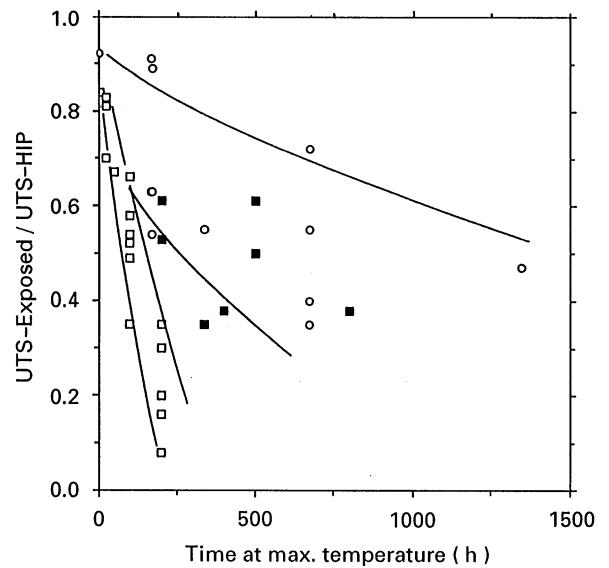


Figure 13 Composite tensile strength, after air exposure, normalized by as-HIP tensile strength, plotted as a function of time at maximum temperature (760 °C). This shows the effect of burying fibre ends and edges within the matrix to protect the SCS-6 fibre coating from oxidation. Key: ○ air-isothermal; □ air-cycled; ■ air-cycled, buried.

amount of fibre breakage, with large (~40%) amounts of broken fibres resulting in composite strengths less than that of the unreinforced matrix.

No significant fibre strength degradation or breakage were detected for samples exposed at 760 °C in argon for up to 1344 h. By comparison, isothermal exposure of Ti-1421/SiC for 672 h at 760 °C in air resulted in an increase in fibre breakage from 5% in the as-HIP sample to 20% after exposure, but no decrease in strength, for the remaining unbroken fibres. The broken fibres were too short to test, and so it is not known if their strength was degraded. Exposure of Ti-1421/SiC for 672 cycles in air at 760 °C resulted in breakage of 85% of the fibres, and a decrease in strength for the remaining unbroken fibres from 4000 MPa as-HIP to 940 MPa after cycling.

Fibre strength loss and increased fibre breakage in cycled samples were probably due to oxidation of the SCS-6 fibre coatings. There was extensive fibre coating oxidation and fibre/matrix interface delamination in samples thermally cycled in air. Propagation of the delamination by thermal stresses resulted in transport of oxygen into the centre of the composite. By comparison, in isothermally exposed samples, only fibres near sample surfaces had oxidized coatings. Since the fibre strength is lower for fibres without the protective coatings [9, 19], coating oxidation probably results in the fibre strength loss observed in the thermally cycled samples. These results are similar to those of Revelos and Smith [17], who cycled samples in air to 815 °C and saw both fibre strength loss and damage to the fibre coating. Increased fibre breakage during thermal cycling may be related to the low fibre strengths, since SCS-6 fibres became susceptible to breakage during HIP or heat treatment when the fibre strengths were 1400–2100 MPa.

3.3.4. Matrix and fibre protection

Use of these composites at elevated temperatures will require that the matrix and fibres be protected from an oxidizing environment. An oxidation-resistant coating on the composite part would be needed to limit surface embrittlement of the matrix. As had been shown, isolating the fibres from direct contact with the environment can be done by burying all fibre ends and lengths within the matrix. However, long times spent at the service temperature can allow sufficient oxygen diffusion through the matrix layer to initiate oxidation of the fibre coating. This suggests that an oxidation-resistant coating on the composite could have some benefit in inhibiting damage to the fibres as well as the matrix.

Some initial research has been published [17, 24] on the properties of coated Ti-1421/SCS-6 composites which were thermally exposed after coating. Coatings which were shown to be protective on monolithic Ti-1421 [24] were unsuccessful when applied to the composites. The large thermal expansion mismatch between the composite and the coatings resulted in cracking of the coatings. The cracks then propagated into the composite, and the tensile properties of the cycled composite were substantially reduced [17]. These results indicate that more work is needed to develop adequate coatings for Ti-base/SiC composites.

4. Conclusions

1. Isothermal and cyclic exposure of longitudinal composites of Ti-1421/SiC at 760 °C in argon caused small losses in room temperature strength and elongation.

2. Exposure of longitudinal composites of Ti-1421/SiC in air at 760 °C resulted in severe losses in strength and elongation. Cycling in air was much more damaging than isothermal exposure.

3. Strength loss in composite samples exposed isothermally in air was attributed to surface embrittlement of the matrix, with the embrittled regions cracking during tensile testing and effectively notching the sample. The decrease in composite strength varied linearly with increasing depth of matrix embrittlement.

4. In samples cycled in air, the effect of surface embrittlement on composite strength was enhanced by cracking of the embrittled region during cycling, followed by propagation of these cracks into the composite.

5. Oxidation of fibre coatings occurred at fibre ends and on fibres exposed to the environment by matrix cracking and fibre layer delamination during cycling. This resulted in a substantial decrease in fibre strength and an increase in fibre breakage during cycling. These factors contributed to the increased loss in strength of the air-cycled samples relative to the isothermally-exposed samples.

6. Use of these composites at 760 °C will require protection of both the fibres and the matrix from the oxidizing environment.

Acknowledgements

The authors would like to thank S. F. Rutkowski for plasma-spraying; A. Barbutto for metallographic sample preparation; C. Canestraro and T. F. Bethel for tensile testing; D. A. Catherine and S. A. Weaver for fibre testing; E. L. Hall and J. Sutliff for the analytical electron microscopy, and M. F. Henry for helpful discussions.

References

1. R. A. WHITE and P. A. SIEMERS, GE CRD Report No. 87CRD145, July 1987.
2. C. G. RHODES and R. A. SPURLING, in "Recent Advances in Composites in the U.S. and Japan", ASTM-STP864, edited by J. R. Vinson and M. Taya (American Society for Testing and Materials, Philadelphia, 1985) p.585.
3. D.S. SHIH and R.A. AMATO, *Scripta Metall.* **24** (1990) p. 2053.
4. P.R. SMITH, F.H. FROES and J.T. CAMMETT, in "Mechanical Behaviour of Metal-Matrix Composites", edited by J.E. Hack and M.F. Amateau (TMS, 1982) p.411.
5. R. A. MACKAY, *Scripta Metall.* **24** (1990) 167.
6. S. M. JENG and J.M. YANG, *J. Mater. Sci.* **27** (1992) 5357.
7. D.R. PANK, A.M. RITTER, R.A. AMATO and J.J. JACKSON, in Proceedings of the Titanium Aluminide Composite Workshop, edited by P.R. Smith, S.J. Balsone and T. Nicholas (1990) p.382.
8. Y-W. KIM, in Proceedings of the Titanium Aluminide Composite Workshop, edited by P.R. Smith, S.J. Balsone and T. Nicholas (1990) p.416.
9. H.E. DEBOLT, R. J. SUPLINSKAS, J.A. CORNIE, T.W. HENZE and A.H. HAUZE, US Patent No. 4 340 636 (1982).
10. A.M. RITTER, E. L. HALL and N. LEWIS, in Materials Research Society Symposium Proceedings, Vol. 194 (1990) 413.
11. S.F. BAUMANN, P.K. BRINDLEY and S.D. SMITH, *Met. Trans. A* **21A**, (1990) 1559.
12. E.L. HALL and A.M. RITTER, *J. Mater. Res.* **8** (1993) 1158.
13. A.M. RITTER, F.C. CLARK and P.L. DUPREE, in "Lightweight Alloys for Aerospace Applications II", edited by E.W. Lee and N.J. Kim (TMS, 1991) p.403.
14. P.K. BRINDLEY, S. DRAPER, J. ELDRIDGE, M. NATHAL and S. ARNOLD, *Metall. Trans. A* **23A** (1992) p. 2527.
15. R.A. MACKAY, S.L. DRAPER, A.M. RITTER and P.A. SIEMERS, *ibid.*, in press.
16. S.M. RUSS, *Met. Trans. A* **21A** (1990) 1595.
17. W.C. REVELO and P.R. SMITH, *ibid.* **23A** (1992) 587.
18. P.K. BRINDLEY, P.A. BARTOLOTTA and R.A. MACKAY, in Proceedings of the 2nd Annual HITEMP Review (NASA Lewis Research Center, Cleveland, OH, 1989).
19. A.M. RITTER and P.L. DUPREE, *Scripta Metall. Mater.* **27** (1992) p. 827.
20. R.N. SHENOY, J. UNNAM and R.K. CLARK, *Oxid. Met.* **26** (1986) 105.
21. S.J. BALSONE, in "Oxidation of High-Temperature Intermetallics", edited by T. Grobstein and J. Doychak, (TMS, 1989) p.219.
22. M.R. EGGLESTON, PhD thesis, Rensselaer Polytechnic Institute, Troy NY (1993).
23. G. DAS and F.W. VAHLIDIEK, in "Interfaces in Metal-Ceramic Composites", edited by R.Y. Lin, R.J. Arsenault, G.P. Martins and S.G. Fishman (TMS, 1989) p.59.
24. W.J. BRINDLEY, J.L. SMIALEK and M.A. GEDWILL, in Proceedings of the 5th Annual HITEMP Review (NASA Lewis Research Center, Cleveland, OH, 1992) p. 41-1.

Received 18 February 1994
and accepted 16 August 1995